



# Time-resolved spectroscopy of Fe<sup>3+</sup> *d-d* transition in bulk ZnSe polycrystal

KYUNG A JEONG,<sup>1</sup> SEONG KU LEE,<sup>2</sup> AND NOSOUNG MYOUNG<sup>2,\*</sup> 

<sup>1</sup>Department of Physics, Chosun University, Gwangju, 61451, South Korea

<sup>2</sup>Advanced Photonics Research Institute, GIST, Gwangju, 61005, South Korea

\*nsmyoung@gist.ac.kr

**Abstract:** We report temperature dependent time-resolved photoluminescence studies of Fe<sup>3+</sup> in ZnSe polycrystals over 10–300 K temperature ranges fabricated by the post growth thermal diffusion technique. The *d-d* transitions of Fe<sup>3+</sup> assigned to the <sup>4</sup>T<sub>2</sub>(G)→<sup>6</sup>A<sub>1</sub>(S) and <sup>4</sup>T<sub>1</sub>(G)→<sup>6</sup>A<sub>1</sub>(S) transitions are clearly identified at 528 and 627 nm, respectively, at 10 K. The observed emission peaks in the near bandgap region are red-shifted from 439 to 463 nm as the temperature increases, resulting in a temperature coefficient of 10.21×10<sup>-4</sup> eV/K and Debye temperature = 336 K fitted by the Varshni equation. The radiative lifetime at 528 nm by time-resolved photoluminescence is evaluated as τ<sub>rad</sub> = 774 ± 4 ps, activation energy (ΔE<sub>a</sub>) = 717.2 cm<sup>-1</sup>, and relaxation time rate (1/W<sub>0</sub>) = 3.1 ps.

© 2019 Optical Society of America under the terms of the [OSA Open Access Publishing Agreement](#)

## 1. Introduction

Transition metals (TMs) doped wide bandgap II–VI semiconductor materials (ZnSe, ZnTe, etc.) are of particular interest owing to their electrical and optical properties [1–5]. Recently, various types of TMs or rare-earth ions doped ZnSe (bulk and nanostructures) have been characterized extensively to enhance their efficiency for laser and solar cell applications [6–8]. Intensive studies on nano-sized zinc chalcogenides doped with TMs (such as Cu and Mn) in the view of their potential for optoelectronic devices have been widely conducted in the visible spectral ranges. For dopant ions like Cu<sup>2+</sup> in ZnSe, the characteristic near band edge emission shifts from 380 to 430 nm while a longer visible emission band is revealed from 400 to 500 nm depending on the particle sizes [9–11]. For Mn<sup>2+</sup> ions [12–14], the emission band has been found near 560 nm (<sup>4</sup>T<sub>1</sub>→<sup>6</sup>A<sub>1</sub>) and 600–640 nm (assigned to a self-activated luminescence). These TM doped nanoparticles exhibit high efficiency and high-temperature stability, as well as long photoluminescence lifetimes. Likewise, for bulk crystals, the development of TM-doped II–VI chalcogenides has been well demonstrated by various fabrication techniques, such as hot isostatic pressing (HIP) [15], chemical vapor deposition (CVD) [16], physical vapor transport (PVT) [17,18], and post-growth thermal diffusion [3,4,19]. However, the presence of TMs and possible energy transfer between different charge states in both nanoparticles and bulk crystals still give rise to difficulties in controlling the optical properties (ultimately decreasing the luminescence efficiency). In the ZnSe polycrystals, the divalent TM ions (for example, Fe<sup>2+</sup> or Cr<sup>2+</sup>) prefer to substitute into the tetrahedrally coordinated Zn<sup>2+</sup> site leading to the middle infrared emission. However, these TM ions are typically known as deactivators of visible luminescence [20,21]. A deep impurity level of TM ions may act as a carrier trapping in the band gap leading the stable charge state of Fe in ZnSe to the Fe<sup>2+</sup>. Concurrently, although many studies on trivalent iron ions in II–VI materials focused on understanding the controversial origin of mechanisms, tremendous efforts have also been devoted to the explanation. For instance, for the trivalent TM ions in zinc chalcogenide crystals, the single positive charge state Fe<sup>3+</sup> and the associated charge transfer processes in the ZnS lattice have been studied through electron spin resonance (ESR) measurement [22].

This study, to the best of our knowledge, is the first time an analysis of the spectroscopic characteristics of  $\text{Fe}^{3+}$  ions in bulk ZnSe polycrystals is demonstrated. Although an extensive study was conducted on bulk Fe:ZnSe in the visible spectral ranges, the existence or optical properties of  $\text{Fe}^{3+}$  ions in ZnSe polycrystals were not clearly reported. Therefore, we report a comprehensive investigation of the trivalent iron cation in ZnSe polycrystal using the temperature dependence of photoluminescence (PL) and time-resolved photoluminescence (TRPL) experiments.

## 2. Materials and methods

The iron thin films on a host crystal, ZnSe ( $10 \times 10 \times 3 \text{ mm}^3$ ), were deposited by electron-beam evaporation of high-purity (99.9%) Fe pellets. Prior to the deposition of the iron thin film, the ZnSe polycrystals were cleaned with 9.5% hydrochloric acid, 5% KOH, acetone, and methanol solutions for the removal of a possible oxide layer, and then washed with distilled water. The iron thin film deposited ZnSe host crystals were then annealed in quartz ampoules ( $< 10^{-4}$  torr) at  $950^\circ\text{C}$  for two weeks. The Fe:ZnSe samples with low Fe concentration of  $2.69 \times 10^{18} \text{ cm}^{-3}$  were prepared for spectroscopic analysis to avoid the influence of nonradiative relaxation and provide minimal distribution of concentration gradient in the host material. The iron concentration in ZnSe was evaluated using the absorption cross-section,  $\sigma_{ab} = 0.65 \times 10^{-18} \text{ cm}^{-2}$  at  $2.698 \mu\text{m}$  [23].

The optical absorption was recorded by UV-visible spectrophotometer (JASCO, V-570) in the wavelength of 400 to 750 nm at 300 K. The PL and TRPL measurements were conducted through second harmonic generation at 400 nm of a mode-locked Ti:sapphire laser (Chameleon Ultra II, Coherent) as an excitation source (3.087 eV, well above the band gap of Fe doped ZnSe even at low temperatures) in the range of 10–300 K within a helium closed cycle cryostat. For PL kinetics measurement, the excitation pulse frequency was decreased by pulse picker (9200 series, Coherent Inc.) to a repetition rate of 3.6 MHz with a pulse duration of 150 fs. The radiation of PL was focused to the entrance slit of a 300 mm spectrograph (Acton SpectraPro 2300i, Princeton Instruments) with a spectral resolution of approximately 1 nm. Then, the TRPL was carefully monitored using a picosecond streak camera (C11200, Hamamatsu Photonics). The dynamic range of streak camera detector can allow in a temporal resolution close to 20 ps.

## 3. Results and discussion

In Fig. 1, the absorption bands of  $\text{Fe}^{3+}$  ions in ZnSe bulk crystals at room temperature are not clearly observed due to the short absorption band and strong emission in the trap state of  $\text{Fe}^{2+}$  ions. The inserted figure indicates the full absorption spectrum of the corresponding  ${}^5\text{E} \rightarrow {}^5\text{T}_2$  vibronic transition of  $\text{Fe}^{2+}$  ions ranging from 2200 to 5000 nm by FTIR (Fourier Transform Infrared) spectroscopy (FTIR-4200, JASCO) in ambient air. The dominant near band edge emission from both bulk ZnSe and Fe:ZnSe occurs near 460 nm (2.7 eV). The iron plays a role as electron trapping center, resulting in nonradiative recombination. We also confirmed a relatively weak, broad emission band from 500 to 650 nm (peak at 1.965 eV corresponding to  ${}^4\text{T}_1 \leftrightarrow {}^6\text{A}_1$ ) due to the donor-acceptor pair (DAP) recombination transition at room temperature [20].

A schematic energy level diagram for  $\text{Fe}^{3+}$  ions in ZnSe is illustrated in Fig. 2(a) and the temperature-dependent PL spectra are recorded (Fig. 2(b)) in the range of 450–700 nm using an excitation wavelength of 400 nm. In Fig. 2(a), the iron-related recombination processes form deep energy levels in the forbidden gap with the  ${}^6\text{S}$  ground state ( ${}^6\text{A}_1(\text{S})$ ),  ${}^4\text{T}_1(\text{G})$  as the first excited state, and  ${}^4\text{T}_2(\text{G})$  as the second excited state for the  $\text{Fe}^{3+}$  charge state. In Fig. 2(b), the first strong emission band at 440 nm is associated with the free exciton recombination process at 10 K (which is not considered in our discussion here), which is a typical emission characteristic for high-purity ZnSe. The second and third emission peaks at 528 nm and 627 nm are incorporated into  $\text{Fe}^{3+}$   $d-d$  transition measured from 10–300 K. In their PL spectra, the three emission peaks correspond to previous reports [24]. The assigned  $\text{Fe}^{3+}$  transition, absorption, and emission bands are given in Table 1. The temperature dependence of the PL emission measurement

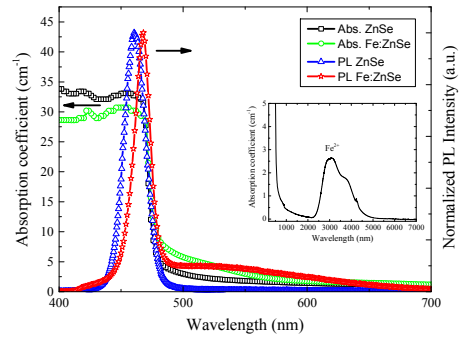


**Fig. 1.** Room temperature absorption and PL spectra of Fe doped ZnSe bulk crystal; (inset) absorption spectrum of  $\text{Fe}^{2+}:\text{ZnSe}$ .

shows the mechanisms of the PL quenching processes caused by the nonradiative carrier loss. In addition, the temperature-dependent PL intensities of 528 nm and 627 nm (at 10 K) bands indicate that the structural defects during the high temperature annealing process tends to quench as temperature increases.

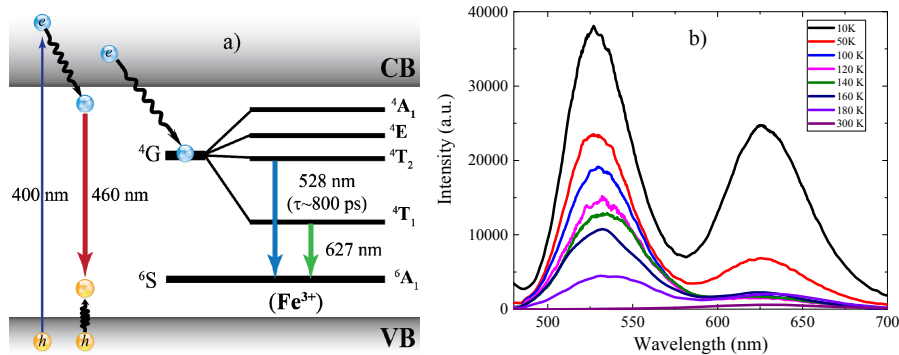


**Fig. 2.** (a) Schematic of possible excited state absorption and emission, and (b) temperature dependence of PL in  $\text{Fe}:\text{ZnSe}$ .

**Table 1. Assigned transitions and absorption/emission peaks at 10 K**

Band Transitions	Absorption (nm) [25]	PL observed (nm)
${}^6\text{A}_{1g}(\text{S}) \leftrightarrow {}^4\text{T}_{2g}(\text{D})$	420	439 (460) <sup>a</sup>
${}^6\text{A}_{1g}(\text{S}) \leftrightarrow {}^4\text{T}_{2g}(\text{G})$	518	528 (552) <sup>a</sup>
${}^6\text{A}_{1g}(\text{S}) \leftrightarrow {}^4\text{T}_{1g}(\text{G})$	610, 690	627

<sup>a</sup> Measured at 300 K

The temperature dependence of the averaged PL peak energies over ten points in  $\text{Fe}:\text{ZnSe}$  polycrystals is shown in Fig. 3. We found that the dominant first peak of band-edge emission red-shifts from 2.82 to 2.67 eV, accompanied by two band emissions, one (D1) ranges from 2.35 to 2.24 eV, and the other (D2) from 1.97 to 1.94 eV as temperature increases. For donor-bound excitonic emission in the band-edge [26], the emission and the PL peak energy decrease abruptly as temperature increases. When the temperature increases from 10 to 80 K for the D1 band, the peak energy slightly decreases, while the peak energy dramatically drops, but not for the PL intensities. Meanwhile, the discrete and minute PL peak shifts of the D2 band are obtained. We

believe that this is the result of the recombination of an electron from the relaxed state to the valence band. The experimental data is fitted using a relation for the variation of the energy gap,  $E_g(T)$ , by the Varshni's empirical equation [27].

$$E_g(T) = E_g(0) - \alpha \frac{T^2}{T + \beta} \quad (1)$$

where  $E_g(0)$  is the band gap energy at 0 K, and  $\alpha$  and  $\beta$  are fitting constants of various conventional materials as a function of temperature. It is known that the value of  $\beta$  is generally related to the Debye temperature. The evaluated parameters are listed in Table 2. Pejova et al. [28] reported that the value of  $\alpha$  for ZnSe nanoparticles is twice larger than the value reported by Novoselova [29]. However, the extracted  $\beta$  value from empirical data is significantly small compared to the two groups since the transition metals doped in ZnSe may require optical phonons at a lower frequency and therefore require smaller activation energy than a pure ZnSe crystal. In addition, the temperature dependence of the peak energy shows the well-known S-shaped behavior which is an indicator of the inhomogeneous distribution of Fe in ZnSe analogous to that in the InGaN system [30]. We believe that the potential fluctuations caused by the inhomogeneous Fe compositional fluctuation have a strong influence on S-shaped PL shift with increasing temperature.

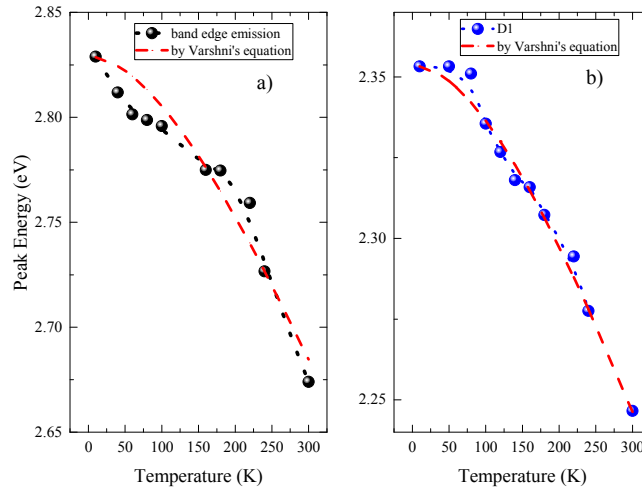


**Fig. 3.** (a) Temperature-dependent PL peak energies of donor-bound excitonic emission in near band edge, and (b) D1 band fitted by the Varshni equation (dotted lines).

**Table 2. Parameters estimated by the Varshni equation.**

Parameters	Units	Band-edge emission			D1
		Observed	by Pejova	by Novoselova	
$E_g(10)$	eV	2.82	3.229	2.82	2.35
$\alpha$	$\times 10^{-4}$ , eV/K	10.2	8.2	4.5	7.9
$\beta$	K	336	398.9	400	367

Here, we also conducted TRPL measurements of  $\text{Fe}^{3+}$  ions in ZnSe polycrystals for different temperatures since these provide important information on the nature of electronic states and recombination modes in Fe:ZnSe. Figure 4 shows the temperature-dependent PL lifetime of band-edge emission of Fe:ZnSe from 10 to 300 K. As shown in Fig. 4(b), the lifetime is almost constant as temperature increases from 10 to 60 K since the fast components of a lifetime up

to 100 K are close to the limit of our time resolution. However, the average lifetime varies significantly with temperature and increases continuously up to 240 K due to the thermal activation of the localized excitons into free excitons [31]. To estimate the PL recombination, the data is fitted by the bi-exponential decay function as shown in Fig. 4(b). The first lifetime term may originate from the electron-hole recombination after excitation in the internal states while the second one is due to the localization process of the exciton. The decay lifetimes of the band-edge emission at 440 nm increase with respect to temperature, which is analogous to the trend previously reported [32].

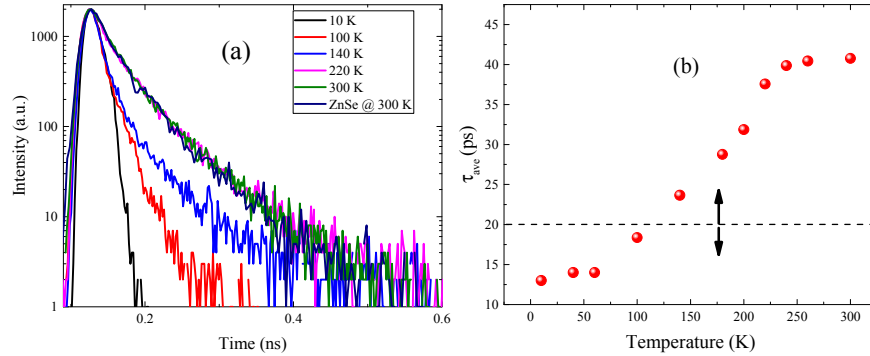


**Fig. 4.** (a) Temperature-dependent kinetics of luminescence and (b) average relaxation time for band-edge emission.

To the best of our knowledge, the temperature-dependent PL lifetime of  $\text{Fe}^{3+}$  ions (D1 emission band) in Fe:ZnSe sample is reported for the first time in Fig. 5. Due to the limitation of low emission intensity signals at temperatures higher than 200 K, the data collected ranged from 10 to 200 K. All PL decay exhibits single exponential behavior. In the temperature range of 10–100 K, the luminescence lifetime is constant at  $774 \pm 4$  ps ( $\tau_{rad}$ ) and then it decreases with temperature due to the thermally activated non-radiative decay. The empirical data of nonradiative process associated with the thermally activated radiationless processes is analyzed by the following equation [33]

$$\frac{1}{\tau(T)} = \frac{1}{\tau_{rad}} + W_{NR} \quad (2)$$

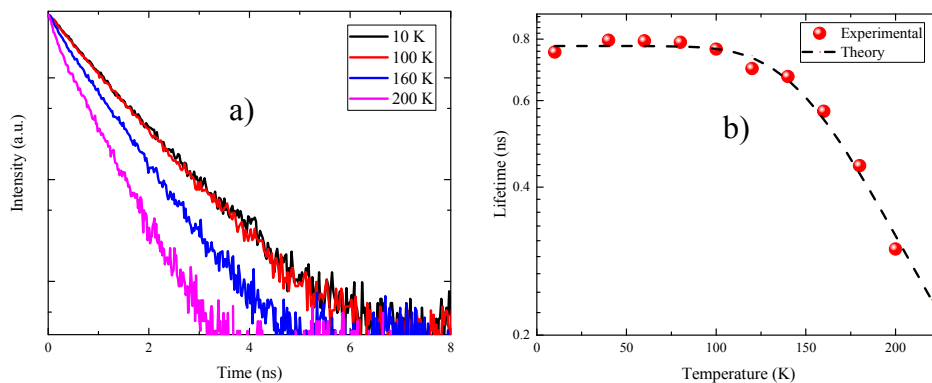


**Fig. 5.** (a) Temperature-dependent luminescence lifetime of D1 band, and (b) fitted curve for the evaluation of thermally activated radiationless transitions.

where  $\tau_{rad}$  is the radiative lifetime, and the non-radiative transition rate ( $W_{NR}$ ) given by

$$W_{NR} = W_0 e^{-\frac{\Delta E_a}{k_B T}} \quad (3)$$

where  $W_0$  is the initial frequency recognized from the effective vibration frequency, and  $\Delta E_a$  is the energy difference (activation energy). The temperature dependent average PL lifetimes under resonant excitation can be well fitted resulting in  $\Delta E_a = 717.2 \text{ cm}^{-1}$  and  $1/W_0 = 3.1 \text{ ps}$ . Furthermore, the extrapolated curve fitting allow us to estimate the PL lifetime as  $\tau = 86 \text{ ps}$  at 300 K.

#### 4. Conclusions

In conclusion, the empirical study of the temperature-dependent time-resolved PL and the radiative recombination processes of  $\text{Fe}^{3+}$  ion in ZnSe polycrystals were reported. The iron-related recombination processes from deep energy levels in the forbidden gap have been investigated by the energy levels with  ${}^6\text{S}$  ground state,  ${}^4\text{T}_1(\text{G})$  as the first excited state, and  ${}^4\text{T}_2(\text{G})$  as the second excited state for  $\text{Fe}^{3+}$  charge state, as well as the band-edge emission as a function of temperature. The radiative lifetime of the  ${}^4\text{T}_2 \leftrightarrow {}^6\text{A}_1$  transition of trivalent Fe ions in the  $\text{Fe}^{2+}:\text{ZnSe}$  crystal was estimated from spectroscopic measurements as  $\tau_{rad} = 774 \text{ ps}$ . The luminescence lifetime of  $\text{Fe}^{3+}$  ions was thermally quenched at temperature of 60 K and higher. Results of TRPL experiments were used to estimate the room temperature luminescence lifetime for the  ${}^4\text{T}_2 \leftrightarrow {}^6\text{A}_1$  transition to be 86 ps through extrapolation of the data. We expect that the spectroscopic investigations of TMs doped bulk ZnSe polycrystals might provide an experimental reference for the fundamental physical properties (for instance, transport properties) and device applications.

#### Funding

National Research Foundation of Korea (NRF) (2016M2B2A4911131, 2017R1D1A1B03031753); Gwangju Institute of Science and Technology (GIST).

#### Acknowledgments

This research was supported by the Basic Science Research Program through the National Research Foundation of Korea (NRF) funded by the Ministry of Education (2017R1D1A1B03031753), national nuclear R&D program through the National Research Foundation of Korea (NRF) grant funded by the Korea government (MSIP) (2016M2B2A4911131), and the ‘‘Research on Advanced Optical Science and Technology’’ grant funded by the GIST in 2019. Special thanks are due to Dr. Sang-Youp Yim for the assistance with the TRPL measurement.

#### References

1. R. Heitz, A. Hoffmann, and I. Broser, ‘‘ $\text{Fe}^{3+}$  center in ZnO,’’ *Phys. Rev. B* **45**(16), 8977–8988 (1992).
2. D. J. Norris, N. Yao, F. T. Charnock, and T. A. Kennedy, ‘‘High-Quality Manganese-Doped ZnSe Nanocrystals,’’ *Nano Lett.* **1**(1), 3–7 (2001).
3. N. Myoung, V. V. Fedorov, S. B. Mirov, and L. Wenger, ‘‘Temperature and concentration quenching of mid-IR photoluminescence in iron doped ZnSe and ZnS laser crystals,’’ *J. Lumin.* **132**(3), 600–606 (2012).
4. N. Myoung, D. Martyskhin, V. Fedorov, and S. Mirov, ‘‘Mid-IR lasing of iron-cobalt co-doped ZnS(Se) crystals via Co-Fe energy transfer,’’ *J. Lumin.* **133**, 257–261 (2013).
5. M. Luo, N. C. Giles, U. N. Roy, Y. Cui, and A. Burger, ‘‘Energy transfer between  $\text{Co}^{2+}$  and  $\text{Fe}^{2+}$  ions in diffusion-doped ZnSe,’’ *J. Appl. Phys.* **98**(8), 083507 (2005).
6. N. Myoung, J. Park, A. Martinez, J. Peppers, S. Yim, W. Han, V. Fedorov, and S. Mirov, ‘‘Mid-IR spectroscopy of Fe:ZnSe quantum dots,’’ *Opt. Express* **24**(5), 5366–5375 (2016).
7. M. Eskandari and V. Ahmadi, ‘‘Treatment effects of ZnO and Al:ZnO photoanodes on short-circuit photocurrent and open-circuit photovoltage of quantum dot sensitized solar cell using Ag nanoparticles,’’ *Electrochim. Acta* **165**, 239–246 (2015).

8. J. Wei, K. Li, J. Chen, J. Zhang, and R. Wu, "Synthesis and photoluminescence of semiconductor ZnSe hollow microspheres by two-sourced evaporation," *J. Alloys Compd.* **531**, 86–90 (2012).
9. J. F. Suyver, T. van der Beek, S. F. Wuister, J. J. Kelly, and A. Meijerink, "Luminescence of nanocrystalline ZnSe:Cu," *Appl. Phys. Lett.* **79**(25), 4222–4224 (2001).
10. M. Godlewski, W. E. Lamb, and B. C. Cavenett, "ODMR investigations of the nature of copper-green and copper-red PL bands in ZnSe," *J. Lumin.* **24-25**(25), 173–176 (1981).
11. G. Jones and J. Woods, "The luminescence of self-activated and copper-doped zinc selenid," *J. Lumin.* **9**(5), 389–405 (1974).
12. J. F. Suyver, S. F. Wuister, J. J. Kelly, and A. Meijerink, "Luminescence of nanocrystalline ZnSe:Mn<sup>2+</sup>," *Phys. Chem. Chem. Phys.* **2**(23), 5445–5448 (2000).
13. M. A. Hines and P. Guyot-Sionnest, "Bright UV-blue luminescent colloidal ZnSe nanocrystals," *J. Phys. Chem. B* **102**(19), 3655–3657 (1998).
14. D. F. Crabtree, "Luminescence, optical absorption, and ESR of ZnS-Se:Mn," *Phys. stat. sol. (a)* **22**(2), 543–552 (1974).
15. R. W. Stites, S. A. McDaniel, J. O. Barnes, D. M. Krein, J. H. Goldsmith, S. Guha, and G. Cook, "Hot isostatic pressing of transition metal ions into chalcogenide laser host crystals," *Opt. Mater. Express* **6**(10), 3339–3353 (2016).
16. V. A. Akimov, A. A. Voronov, V. I. Kozlovskii, Y. V. Korostelin, A. I. Landman, Y. P. Podmar'kov, and M. P. Frolov, "Efficient lasing in a Fe<sup>2+</sup>:ZnSe crystal at room temperature," *Quantum Electron.* **36**(4), 299–301 (2006).
17. C. Su, S. Feth, M. P. Volz, R. Matyi, M. A. George, K. Chattopadhyay, A. Burger, and S. L. Lehoczky, "Vapor growth and characterization of Cr-doped Znse crystals," *J. Cryst. Growth* **207**(1-2), 35–42 (1999).
18. V. I. Kozlovskiy, V. A. Akimov, M. P. Frolov, Yu. V. Korostelin, A. I. Landman, V. P. Martovitsky, V. V. Mislavskii, Yu. P. Podmar'kov, Ya. K. Skasyrsky, and A. A. Voronov, "Room-temperature tunable mid-infrared lasers on transition-metal doped II-VI compound crystals grown from vapor phase," *Phys. Status Solidi B* **247**(6), 1553–1556 (2010).
19. N. Myoung, D. V. Martyshekin, V. V. Fedorov, and S. B. Mirov, "Energy scaling of 4.3 μm room temperature Fe:ZnSe laser," *Opt. Lett.* **36**(1), 94–96 (2011).
20. M. Surma, M. Godlewski, and T. P. Surkova, "Iron and chromium impurities in ZnSe as centers of nonradiative recombination," *Phys. Rev. B* **50**(12), 8319–8324 (1994).
21. M. Chen, C. Hu, W. Li, H. Kou, J. Li, Y. Pan, and B. Jiang, "Cr<sup>3+</sup> in diffusion doped Cr<sup>2+</sup>:ZnS," *Ceram. Int.* **40**(5), 7573–7577 (2014).
22. M. Godlewski and A. Zakrzewski, "Photo-ESR studies of the iron photo-neutralisation process in the ZnS lattice," *J. Phys. C: Solid State Phys.* **18**(36), 6615–6625 (1985).
23. J. J. Adams, C. Bibeau, R. H. Page, D. M. Krol, L. H. Furu, and S. A. Payne, "4.0-4.5 μm lasing of Fe:ZnSe below 180 K, a new mid-infrared laser material," *Opt. Lett.* **24**(23), 1720–1722 (1999).
24. L. Hou, C. Chen, L. Zhang, Q. Xu, X. Yang, M. Farooq, J. Han, R. Liu, Y. Zang, L. Shi L, and B. Zou, "Spin-related micro-photoluminescence in Fe<sup>3+</sup> doped ZnSe nanoribbons," *Appl. Sci.* **7**(1), 39 (2017).
25. S. M. Begum, M. C. Rao, Y. Aparna, P. S. Rao, and R. Ravikumar, "Spectroscopic investigations of Fe<sup>3+</sup> doped poly vinyl alcohol (PVA) capped ZnSe nanoparticles," *Spectrochim. Acta, Part A* **98**, 100–104 (2012).
26. M. Isshiki, K. Masumoto, W. Uchida, and S. Satoh, "Estimation of the donor concentration in ZnSe from the emission related to donor bound excitons," *Jpn. J. Appl. Phys.* **30**(Part 1), 515–516 (1991).
27. Y. P. Varshni, "Temperature dependence of the energy gap in semiconductors," *Physica* **34**(1), 149–154 (1967).
28. B. Pejova, B. Abay, and I. Bineva, "Temperature dependence of the band-gap energy and sub-band-gap absorption tails in strongly quantized ZnSe nanocrystals deposited as thin film," *J. Phys. Chem. C* **114**(36), 15280–15291 (2010).
29. A. B. Novoselova, *Physical and Chemical Properties of Semiconductors: A Handbook* Nauka, ed. (Springer, 1978).
30. Y. Cho, G. H. Gainer, A. J. Fischer, and J. J. Song, "'S-shaped' temperature-dependent emission shift and carrier dynamics in InGaN/GaN multiple quantum wells," *Appl. Phys. Lett.* **73**(10), 1370–1372 (1998).
31. C. Weisbuch, R. Dingle, A. Gossard, and W. Wiegmann, "Optical characterization of interface disorder in GaAs-Ga<sub>1-x</sub>Al<sub>x</sub> as multi-quantum well structures," *Solid State Commun.* **38**(8), 709–712 (1981).
32. G. Yang, Z. Ma, H. Zhong, S. Zou, C. Chen, J. Han, and B. Zou, "Probing exciton move and localization in solution-grown colloidal CdSe<sub>x</sub>S<sub>1-x</sub> alloyed nanowires by temperature- and time-resolved spectroscopy," *J. Phys. Chem. C* **119**(39), 22709–22717 (2015).
33. B. Henderson and R. H. Bartran, *Crystal-Field Engineering of Solid-State Laser Materials* (Cambridge University Press, 2000), p. 177 .